848. Nonlinear free vibration analysis of the functionally graded beams

H. Askari[1], D. Younesian[2], Z. Saadatnia[3], E. Esmailzadeh[4]
[1, 2, 3]Center of Excellence in Railway Transportation, School of Railway Engineering
Iran University of Science and Technology, Narmak, Tehran, 16846, Iran
[4]Faculty of Engineering and Applied Science, University of Ontario
Institute of Technology, Oshawa, Ontario, Canada
E-mail: [1]*askari.iust@gmail.com*, [2]*younesian@iust.ac.ir*, [3]*zia_saadat@rail.iust.ac.ir*, [4]*Ezadeh@uoit.ca*

(Received 10 April 2012; accepted 4 September 2012)

Abstract. Nonlinear natural oscillations of beams made from functionally graded material (FGM) are studied in this paper. The equation of motion is derived according to the Euler-Bernoulli beam theory and von Karman geometric nonlinearity. Subsequently, Galerkin's solution technique is applied to obtain the corresponding ordinary differential equation (ODE) for the FGM beam. This equation represents a kind of a nonlinear ODE containing quadratic and cubic nonlinear terms. This nonlinear equation is then solved by means of three efficient approaches. Homotopy perturbation method is applied at the first stage and the corresponding frequency-amplitude relationship is obtained. Frequency-amplitude formulation and Harmonic balance method are then employed and the consequent frequency responses are determined. In addition, Parameter Expansion Method is utilized for evaluating the nonlinear vibration of the system. A parametric study is then conducted to evaluate the influence of the geometrical and mechanical properties of the FGM beam on its frequency responses. Different types of material properties and boundary conditions are taken into account and frequency responses of the system are evaluated for different gradient indexes. The frequency ratio (nonlinear to linear natural frequency) is obtained in terms of the initial amplitude and compared for different materials and end conditions.

Keywords: frequency-amplitude relationship, FGM beams, nonlinear vibration, Euler-Bernoulli beam.

Introduction

The idea of functionally gradient materials was initiated by a team of researchers in Japan to avoid effect of thermal stresses. Thermal stresses are created as a result of direct bonding of metals and ceramics in high temperature applications. They can generate interface cracks, debonding at hetero-interfaces, and result in delimitation of the over-layer of the ceramics. Initially and originally, concept of FGM materials was employed for creating fuselage exterior and engine materials. Then, it was utilized for improving the figure of merit of thermoelectric materials [1]. FGMs were also employed in optoelectronics systems such as antireflective layers, fibers, GRIN lenses, and other passive elements made from dielectrics [2]. This concept was then widely employed to improve various mechanical and electrical systems. For instance, graded thermoelectric and dielectric elements [3], graded composite electrodes for solid oxide fuel cells [4], and piezoelectrically graded materials were employed for broadband ultrasonic transducers [5]. This idea was also applied for high current connectors [6]. Recently, vibration and dynamic analysis of functionally graded materials has attracted several researchers. Vibration of FGM cylindrical shells was analyzed by Loy et al. [7] in 1995. They have employed Love's shell theory and Rayleigh–Ritz method for obtaining strains displacements and eigenvalue governing equation. Dynamic response of initially stressed functionally graded rectangular thin plates was investigated by Yang and Shen [8]. The results of investigation are presented in Table 1. They conducted a parametric study on the effects of constituent volume fraction index, foundation stiffness, plate aspect ratio, the shape and duration of impulsive load as well as the initial membrane stresses on the dynamic response of the FGM plates. Large amplitude vibration of thermo-electro-mechanically stressed FGM laminated plates was analyzed by Yang et al. [9]. They used differential quadrature method for predicting dynamic behavior of the laminated rectangular plates with two opposite clamped edges. Nonlinear vibration of initially stressed functionally graded plates was studied by Chen et al. [10]. They employed Galerkin's solution method in conjunction with the Runge-Kutta integration technique to obtain frequency responses. Vibration of a simply supported functionally graded piezoelectric rectangular plate was investigated by Zhong and Yu [11]. The exact frequency equations of free vibration were determined for several numerical examples. Vibration of a functionally graded piezoelectric cylindrical actuator based on elastic membrane and shell theories was studied by Zhang et al. [12]. The present paper is aimed at analysis of nonlinear oscillations of FGM beams for different conditions. Linear vibration analysis of FGM beams has been extensively addressed in the literature. For instance, Lu and Chen studied free vibration of orthotropic functionally graded beams. They employed hybrid state-space/differential quadrature method for obtaining a semi analytical solution [13]. Wei et al. [14] provided an analytical approach to solve free vibration of a cracked functionally graded beam including axial loading, rotary inertia and shear deformation. Nonlinear dynamic behavior of a functionally graded Timoshenko beam traversed by a moving load was analyzed by M. Sismek [15]. Effects of large deflection, material distribution, traveling speed and excitation frequency on the beam displacement, bending moment were investigated. Pradhan and Murmu [16] employed differential quadrature method and studied thermo-mechanical vibration of a FGM sandwich beam on an elastic foundation. More recently, Ke et al. [17] employed direct numerical integration method and analyzed nonlinear free vibration of a FGM beam with different end supports. Surveying the literature shows that due to the limitation and complexity of the solution procedures, there are very few publications on nonlinear vibrations of FGM beams. Furthermore, a large number of researchers have investigated diverse parameters in FGM structures. Interested readers can study these valuable works for obtaining information about recent trends in analyzing of FGM structures [18-22]. In present study, four straightforward analytical approaches are presented for frequency analysis of the nonlinear FGM beams. Homotopy Perturbation method, frequency amplitude formulation, Harmonic balance method and Parameter expansion method are employed for deriving the natural frequency of the nonlinear FGM beam. Homotopy perturbation method (HPM) is one of the recent and strong methods for solving nonlinear problems, developed by J. H. He [23]. This method has been already employed for different nonlinear equations by a number of researchers [24-26]. Frequency amplitude formulation (FAF) is another strong and straightforward solution technique suggested by J. H. He [27]. Several researchers [28-31] have utilized this method so far to solve nonlinear conservative oscillatory systems such as generalized Duffing equation, relativistic oscillator, Duffing harmonic, and plasma Physics equations. The third solution method i.e. harmonic balance (HBM), is one of the classic and prominent methods for solving nonlinear problems and has been already developed by many researchers [32-34]. Besides, Parameter expansion method is exerted for frequency analyzing of this system. Parameter expansion is a strong method which has been used by several researchers for analyzing various nonlinear systems [35-38]. Furthermore, a number of novel and potent analytical approaches have been recently proposed and applied for solving nonlinear problems [39-42]. In this paper, after derivation of the governing equation of motion for a nonlinear FGM beam, Galerkin technique is applied for extracting the corresponding nonlinear ordinary differential equation. Subsequently, three different approaches (HPM, FAF and HBM) are employed for determination of frequency responses of the FGM beam. A parametric study is carried out and influences of the material property variation index on the frequency responses are studied. Furthermore, different types of boundary conditions are examined, and the consequent natural frequencies of the system are obtained. Frequency ratio for different types of materials and different end conditions are plotted versus the initial amplitude. Eventually, the exact solutions for nonlinear differential equation are numerically obtained and accuracy of the proposed analytical methods is evaluated.

1. Formulation

Geometry of a FGM beam is illustrated in Fig. 1. Nonlinear differential equation of motion is presented for the beam in this section.

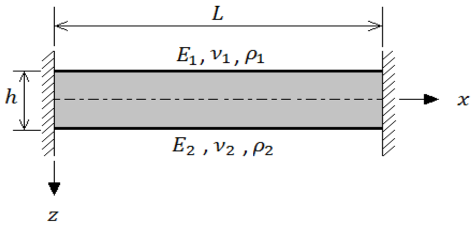

Fig. 1. Geometry of an FGM beam

By using Hamilton's principle, the equations of motion can be derived as [17]:

$$\frac{\partial N_x}{\partial x} = I_1 \frac{\partial^2 U}{\partial t^2}, \tag{1}$$

$$\frac{\partial^2 M_x}{\partial x^2} + \frac{\partial}{\partial x}\left(N_x \frac{\partial W}{\partial x}\right) = I_1 \frac{\partial^2 W}{\partial^2 t}, \tag{2}$$

where the force and bending moment resultants are:

$$N_x = A_{11}[\frac{\partial U}{\partial x} + \frac{1}{2}(\frac{\partial W}{\partial x})^2] - B_{11}\frac{\partial^2 W}{\partial X}, \tag{3a}$$

$$M_x = A_{11}[\frac{\partial U}{\partial x} + \frac{1}{2}(\frac{\partial W}{\partial x})^2] - B_{11}\frac{\partial^2 W}{\partial X}. \tag{3b}$$

The stiffness components and inertia related terms are defined to be:

$$\{A_{11}, B_{11}, D_{11}\} = \int_{-h/2}^{h/2} \frac{E(z)}{1-\upsilon^2}\{1, z, z^2\}dz, \tag{4a}$$

$$I_1 = \int_{-h/2}^{h/2} \rho(z)dz. \tag{4b}$$

If the axial inertia is neglected, Equation (1) gives:

$$N_x = N_{x0} \text{ or } N_{x0} = \frac{A_{11}}{L}\int_0^L [\frac{1}{2}(\frac{\partial W}{\partial X})^2 - \frac{B_{11}}{A_{11}}\frac{\partial^2 W}{\partial x^2}]dx. \tag{5}$$

For beams with immovable ends, integrating (5) with respect to x leads to:

$$0 = [U]_{x=0}^{x=L} = \int_0^L [A_{11}(N_{x0} + B_{11}\frac{\partial^2 W}{\partial x^2}) - \frac{1}{2}(\frac{\partial W}{\partial x})^2]dx. \tag{6}$$

Hence:

$$N_{x0} = \frac{A_{11}}{L}\int_0^L [\frac{1}{2}(\frac{\partial W}{\partial x})^2 - \frac{B_{11}}{A_{11}}\frac{\partial^2 W}{\partial x^2}]. \tag{7}$$

From (3b) and (5), bending moment can be re-expressed in terms of the deflection as:

$$M_x = \frac{B_{11}}{A_{11}}[N_{x0} + B_{11}\frac{\partial^2 W}{\partial x^2}] - D_{11}\frac{\partial^2 W}{\partial x^2}. \tag{8}$$

Combining Equations (1), (2), (5) and (8) yields:

$$\left(\frac{B_{11}^2}{A_{11}}-D_{11}\right)\frac{\partial^4 W}{\partial x^4}+N_{x0}\frac{\partial^2 W}{\partial x^2}=I_1\frac{\partial^2 W}{\partial t^2}. \tag{9}$$

Introducing the following dimensionless quantities [17]:

$$\xi=\frac{x}{L},\ (u,w)=\frac{(U,W)}{h},\ \bar{I}=\frac{I_1}{I_{10}},\ \eta=\frac{h}{L}, \tag{10a}$$

$$(a_{11},b_{11},d_{11})=\left(\frac{A_{11}}{A_{110}},\frac{B_{11}}{hA_{110}},\frac{D_{11}}{A_{110}h^2}\right). \tag{10b}$$

where A_{110} and I_{10} are taken as the values of A_{11} and I_1 of a homogeneous beam. Equation (9) can be reconstructed in dimensionless form as:

$$d_0\eta^2\frac{\partial^4 w}{\partial \xi^4}+\bar{N}_{x0}\frac{\partial^2 w}{\partial \xi^2}=\bar{I}_1\frac{\partial^2 w}{\partial \tau^2}, \tag{11}$$

where:

$$d_0=\frac{b_1^2}{a_{11}}-d_{11},\ \bar{N}_{x0}=a_{11}\eta^2\int_0^1\left[\frac{1}{2}\left(\frac{\partial w}{\partial \xi}\right)^2-\frac{b_{11}}{a_{11}}\frac{\partial^2 w}{\partial \xi^2}\right]d\xi. \tag{12}$$

The first order Galerkin's solution can be expressed as:

$$w(\xi,\tau)=u\ (\tau)\psi(\xi), \tag{13}$$

where $u(\tau)$ is the time dependent function to be determined and $\psi(\xi)$ is the linear fundamental vibration mode. Substituting Eq. (13) into Eq. (11) and applying Galerkin's procedure yield to the corresponding second order nonlinear ordinary differential equation:

$$\ddot{u}+\gamma_a u+\gamma_b u^2+\gamma_c u^3=0, \tag{14}$$

γ_a, γ_b, γ_c have been accordingly defined in Appendix 1.

2. Solution Procedure

We first consider the corresponding auxiliary equations [31]:
for ($u\geq 0$)

$$\ddot{u}+\alpha u+\beta u^2\mathrm{sgn}(u)+\gamma u^3=0, \tag{15}$$

and for ($u\leq 0$)

$$\ddot{u}+\alpha u-\beta u^2\mathrm{sgn}(u)+\gamma u^3=0. \tag{16}$$

Theses auxiliary equations are discussed in Appendix 2.

2. 1. Homotopy Perturbation Method

In Eq. (15), let ω_a be the initial angular frequency. We construct a homotopy of:

$$(1-p)\omega_a(\ddot{u}+\alpha u)+p[\omega^2\ddot{u}+\alpha u+\beta u^2\mathrm{sgn}(u)+\gamma u^3]=0, \tag{17}$$

where $p\in[0,1]$ is an embedding parameter. When $p=0$, Eq. (17) is a simple harmonic equation of:

$$\ddot{u}+\alpha u=0,\quad u(0)=a\quad\text{and}\quad \dot{u}(0)=0. \tag{18}$$

The power series of the homotopy perturbation parameter p is defined to be:

$$u=u_0+pu_1+p^2u_2+\ldots. \tag{19}$$

$$\omega = \omega_a + \omega_1 p + \omega_2 p^2 + ... \tag{20}$$

Substituting Eqs. (19) and (20) into Eq. (17) and equating the terms with the identical powers of the embedding parameter p, we can obtain a series of linear equations. The initial approximate is given by:

$$\ddot{u}_0 + u_0 = 0. \tag{21}$$

With initial conditions $u_0(a) = a$ and $\dot{u}_0(a) = 0$, the first approximation is given by:

$$\omega_a^2(\ddot{u}_1 + \alpha u_1 - \ddot{u}_0 - \alpha u_0) + \omega_0^2 \ddot{u}_0 + \alpha u_0 + \beta u_0^2 \operatorname{sgn}(u) + \gamma u_0^{\ 3} = 0. \tag{22}$$

The solution of Eq. (21) is simply given by:

$$u_0 = a\cos\omega t. \tag{23}$$

Substituting Eq. (23) into Eq. (22) gives:

$$\begin{aligned} \omega_a^2(\ddot{u}_1 + \alpha u_1) = -[-\omega_a^2 a\cos\omega t + \alpha a\cos\omega t + \\ \beta a^2 \operatorname{sgn}(a\cos\omega t)\cos^2\omega t + \gamma a^3 \cos^3 \omega t]. \end{aligned} \tag{24}$$

Using the following expansion:

$$\operatorname{sgn}(\cos\omega t) \approx \frac{4}{\pi}\left(\cos\omega t - \frac{1}{3}\cos(3\omega t) + \frac{1}{5}\cos(5\omega t)\right), \tag{25}$$

and eliminating secular terms in Eq. (24) one can arrive to:

$$\omega_a = \sqrt{\alpha + \frac{3}{4}\gamma a^2 + \frac{8a}{3\pi}\beta}. \tag{26}$$

Likewise, one can take the auxiliary equation (16) and construct a homotopy for the initial angular frequency:

$$(1-p)\omega_b\ (\ddot{u} + \alpha u) + p[\omega^2 \ddot{u} + \alpha u - \beta u^2 \operatorname{sgn}(u) + \gamma u^3] = 0. \tag{27}$$

One can similarly arrive to the following solutions:

$$u_b = b\cos\omega_b t, \tag{28}$$

$$\omega_a = \sqrt{\alpha + \frac{3}{4}\gamma a^2 - \frac{8a}{3\pi}\beta}. \tag{29}$$

2. 2. Harmonic Balance Method

By substituting Eq. (23) into Eq. (15) and implementing the HBM solution steps, we obtain:

$$(-\omega_a^2 + \alpha + \frac{3\gamma}{4}a^2 + \frac{8\beta}{3\pi}a)a\cos(\omega_a t) + \text{Higher order harmonics} = 0. \tag{30}$$

Eliminating coefficient of $a\cos(\omega_a t)$ and solving for ω_a^2, yields:

$$\omega_a = \sqrt{\alpha + \frac{3}{4}\gamma a^2 + \frac{8a}{3\pi}\beta}. \tag{31}$$

Similar procedure is applied to Eq. (16) to reach:

$$(-\omega_b^2 + \alpha - \frac{3\gamma}{4}b^2 + \frac{8\beta}{3\pi}b)b\cos(\omega_b t) + \text{Higher order harmonics} = 0. \tag{32}$$

In the same way one can arrive to:

$$\omega_b = \sqrt{\alpha + \frac{3}{4}\gamma b^2 - \frac{8b}{3\pi}\beta}. \tag{33}$$

Corresponding time responses of Eq. (14) are discussed in Appendix 3.

2. 3. Frequency Amplitude Formulation

According to the standard procedure of the FAF, the trial functions of $u_1(t) = a\cos t$ and $u_2(t) = a\cos\omega t$ are assumed in positive direction. The frequency-amplitude formulation is consequently obtained:

$$\omega^2 = \frac{\omega_1^2 \tilde{R}_2 - \omega_2^2 \tilde{R}_1}{\tilde{R}_2 - \tilde{R}_1}. \tag{34}$$

Substituting the trial functions into Eq. (15) results in the following residuals:

$$R_1(t_1) = \beta(\mathrm{sgn}(a\cos t))\alpha^2\cos^2 t + \gamma a^3\cos^3 t, \tag{35}$$

$$R_2(t_2) = a\cos\omega t\left(\alpha - \omega^2\right) + \left(\mathrm{sgn}(a\cos\omega t)\right)a^2\cos^2\omega t + \alpha a^3\cos^3\omega t. \tag{36}$$

The above residuals can be represented in the forms of following weighted residuals:

$$\tilde{R}_1 = \frac{4}{T_1}\int_0^{T_1/4} R_1 \cos t\,dt = \frac{4}{3\pi}\beta a^2 + \frac{3}{8}\gamma a^3, \tag{37}$$

$$\tilde{R}_2 = \frac{4}{T_2}\int_0^{T_2/4} R_2 \cos\omega t\,dt = \frac{a}{2}\left(\alpha - \omega^2\right) + \frac{4}{3\pi}\beta a^2 + \frac{3}{8}\gamma a^3. \tag{38}$$

After substitution of Eqs. (37)-(38) into Eq. (34) and implementing a number of mathematical simplifications one can reach:

$$\omega_a = \sqrt{\alpha + \frac{8}{3\pi}\beta a + \frac{3}{4}\gamma a^2}\ , \tag{39}$$

$$\omega_b = \sqrt{\alpha - \frac{8}{3\pi}\beta b + \frac{3}{4}\gamma b^2}. \tag{40}$$

As a primary conclusion, it may be emphasized that the three different approaches give the same result for the nonlinear frequency amplitude relationship.

2. 4. Parameter Expansion Method

The new form of Eq. (15) is constructed based on the Parameter Expansion Method as:

$$\ddot{u} + 0\cdot u + 1\cdot\alpha u + 1\cdot\beta u^2\mathrm{sgn}(u) + 1\cdot\gamma u^3 = 0. \tag{41}$$

According to the parameter expansion method, we have:

$$\begin{cases} u = u_0 + \varepsilon u_1 + \varepsilon^2 u_2 + \dots \\ 0 = \omega^2 + \varepsilon\omega_1 + \varepsilon^2\omega_2 + \dots \\ 1 = \varepsilon a_1 + \varepsilon^2 a_2 + \dots \\ 1 = \varepsilon b_1 + \varepsilon^2 b_2 + \dots \\ 1 = \varepsilon c_1 + \varepsilon^2 c_2 + \dots \end{cases} \tag{42}$$

We substitute Eq. (42) into Eq. (43) and then obtain:

$$\begin{aligned} &(\ddot{u}_0 + \varepsilon\ddot{u}_1 + \varepsilon^2\ddot{u}_2 + \dots) + (\omega^2 + \varepsilon\omega_1 + \varepsilon^2\omega_2 + \dots)(u_0 + \varepsilon u_1 + \varepsilon^2 u_2 + \dots) + \\ &(\varepsilon a_1 + \varepsilon^2 a_2 + \dots)u(\varepsilon a_1 + \varepsilon^2 a_2 + \dots)\alpha u + \\ &(\varepsilon b_1 + \varepsilon^2 b_2 + \dots)\beta(u_0 + \varepsilon u_1 + \varepsilon^2 u_2 + \dots)^2\mathrm{sgn}(u_0 + \varepsilon u_1 + \varepsilon^2 u_2 + \dots) + \end{aligned} \tag{43}$$

$$(\varepsilon c_1 + \varepsilon^2 c_2 + \ldots)\gamma(u_0 + \varepsilon u_1 + \varepsilon^2 u_2 + \ldots)^3 = 0.$$

By equating the terms having the same identical powers of ε one can arrive at:

$$\begin{cases} \varepsilon^0 : \ddot{u}_0 + \omega^2 u_0 = 0, \\ \varepsilon^1 : \ddot{u}_1 + \omega^2 u_1 + \omega_1 u_0 + a_1 \alpha u_0 + b_1 \beta u_0^2 \operatorname{sgn}(u_0) + c_1 \gamma u_0^3 = 0. \end{cases} \tag{44}$$

Inserting Eq. (23) into Eq. (44) gives:

$$\ddot{u}_1 + \omega^2 u_1 + \omega_1 a \cos\omega t + a_1 a \cos\omega t + b_1 \beta a^2 \cos^2 \omega t \operatorname{sgn}(a\cos\omega t) \\ + c_1 \gamma a^3 \cos^3 \omega t = 0. \tag{45}$$

By considering the first approximation when $\varepsilon = 1$:

$$\begin{cases} u = u_0 + u_1, \\ a_1 = 1, b_1 = 1, c_1 = 1, \\ 0 = \omega^2 + \omega_1. \end{cases} \tag{46}$$

Using Eqs. (45)-(46) and eliminating secular terms in Eq. (46) we obtain:

$$\omega_a = \sqrt{\alpha + \frac{8a}{3\pi}\beta + \frac{3}{4}\gamma a^2}. \tag{47}$$

By using the same procedure for Eq. (16), Eq. (48) is obtained to be frequency-amplitude relationship:

$$\omega_b = \sqrt{\alpha - \frac{8b}{3\pi}\beta + \frac{3}{4}\gamma b^2}. \tag{48}$$

3. Discussion

In this section, a parametric study is carried out to further investigate how end conditions and type of FGM can influence nonlinear dynamic behavior of the beam. Nonlinear natural frequency to linear one is defined to be the frequency ratio. Values of analytical frequencies are tabulated with respect to the gradient index and various boundary conditions. Fig. 2 presents the frequency ratio for an exponentially varying material property and hinged-hinged boundary conditions. Also, Figs. 3-4 show the frequency ratio for the same material and clamped-clamped and clamped-hinged boundary conditions, respectively.

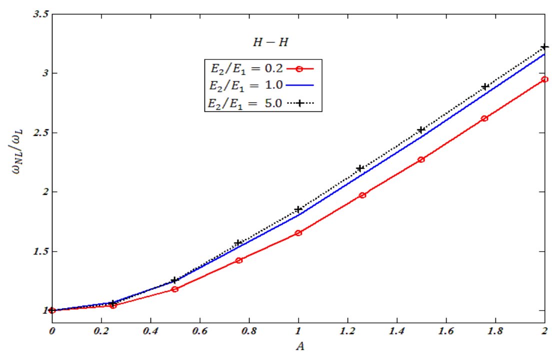

Fig. 2. Frequency ratio *vs*. amplitude for exponentially varying material properties (hinged-hinged boundary condition)

It is observed that frequency ratio increases by increasing the initial amplitude of oscillation. Comparison of Figs. 2-4 indicates that for a given point, the value of the ratio is larger for hinged-hinged boundary condition when compared to other conditions. In other words, natural frequency of a hinged-hinged beam is further influenced in large amplitude vibration. Figs. 5-7 illustrate the same curves for power-law material property distributions.

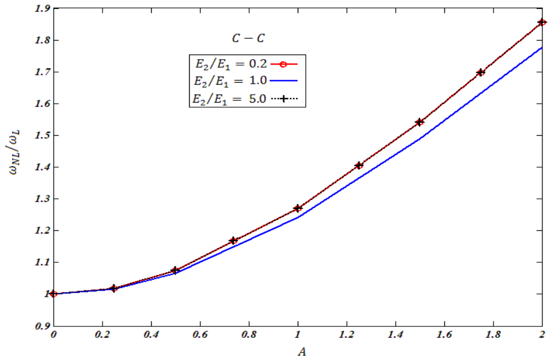

Fig. 3. Frequency ratio vs. amplitude for exponentially varying material properties (clamped-clamped boundary condition)

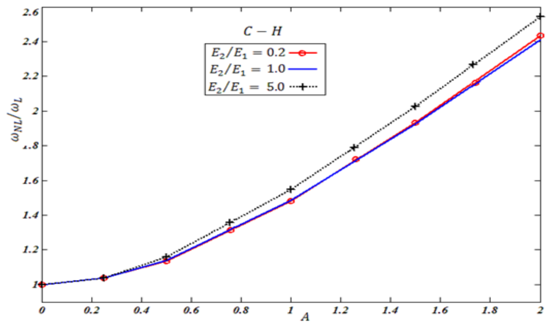

Fig. 4. Frequency ratio vs. amplitude for exponentially varying material properties (clamped-hinged boundary condition)

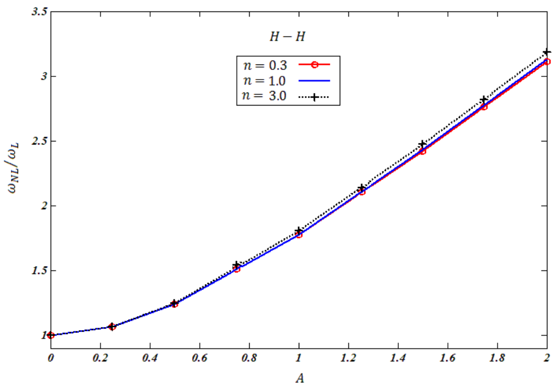

Fig. 5. Frequency ratio vs. amplitude for power-law material property distributions (hinged-hinged boundary condition)

© VIBROENGINEERING. JOURNAL OF VIBROENGINEERING. SEPTEMBER 2012. VOLUME 14, ISSUE 3. ISSN 1392-8716

Again it is observed that for a given point, the frequency ratio is larger for the hinged-hinged boundary conditions. Furthermore, it can be concluded that, for a certain point, by increasing the value of gradient index, the frequency ratio decreases.

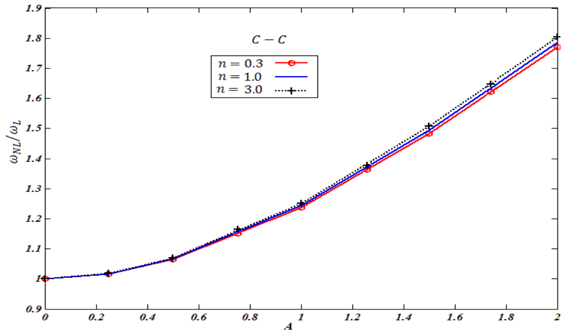

Fig. 6. Frequency ratio vs. amplitude for power-law material property distributions (clamped-clamped boundary condition)

Table 1 lists the values of frequencies for different parameters and boundary conditions. The exact period of the equation response can be obtained by elliptical integration as:

$$T_{ex} = \int_0^a \frac{2dx}{\sqrt{(a^2-x^2)+\frac{2}{3}(a^3-x^3)+\frac{1}{2}(a^4-x^4)}} + \int_0^b \frac{2dx}{\sqrt{(b^2-x^2)+\frac{2}{3}(b^3-x^3)+\frac{1}{2}(b^4-x^4)}}. \quad (49)$$

Table 1. Comparison between exact and approximate nonlinear frequency for A = 1

Exponential/power law	Hinged-Hinged		Clamped-Clamped		Clamped-Hinged	
	ω_{Exact}	$\omega_{Approximate}$ (Relative error %)	ω_{Exact}	$\omega_{Approximate}$ (Relative error %)	ω_{Exact}	$\omega_{Approximate}$ (Relative error %)
$E_2/E_1 = 0.2$	0.29754	0.30035 (0.94727)	0.47993	0.48138 (0.30262)	0.39006	0.39256 (0.64023)
$E_2/E_1 = 1.0$	0.31775	0.32102 (1.02880)	0.49955	0.50084 (0.25796)	0.41018	0.41277 (0.63229)
$E_2/E_1 = 5.0$	0.33162	0.33548 (1.16351)	0.51993	0.5099 (1.092)	0.42712	0.41311 (0.73458)
$n = 0.3$	0.16117	0.16278 (1.00116)	0.25625	0.25691 (0.25372)	0.20945	0.21074 (0.61709)
$n = 1.0$	0.19225	0.19419 (1.00750)	0.30567	0.30647 (0.26237)	0.25002	0.25159 (0.62784)
$n = 3.0$	0.23573	0.23816 (1.03386)	0.37201	0.37303 (0.27324)	0.30545	0.30743 (0.64856)

It is obvious that values of frequencies increase by increasing the gradient index. Frequency value of a certain boundary condition and amplitude for exponential gradient index is larger than power law gradient index. It is also determined that for a given gradient index and amplitude, the value of frequency for the clamped-clamped boundary condition is more than other kinds of boundary conditions. The obtained relative errors disclose the fact that the employed methods all are fairly reliable for nonlinear vibration analysis of a FGM beam with conventional boundary conditions.

Conclusions

Large amplitude vibration of a FGM beam was formulated based on the von Karman theory. Galerkin's method was applied to derive the corresponding nonlinear vibration equation of the system. Three different solution methods, namely homotopy perturbation, frequency amplitude formulation and harmonic balance, were employed to solve the supporting nonlinear differential equation. A comprehensive parametric study was carried out to further identify the natural behavior of the dynamic system. The following conclusions can be listed:
1) For the given initial amplitude, the frequency ratio for a hinged-hinged boundary condition is larger in comparison with the other types of boundary conditions. This means that in this case, the difference between linear and nonlinear natural frequency is enhanced.
2) For the given initial amplitude, increase of value of gradient index leads to frequency ratio increase.
3) By increasing the initial amplitude, the nonlinear natural frequency increases in a hardening pattern.
4) In this dynamic system, Homotopy perturbation method, Harmonic balance method and frequency amplitude formulation give the same result in terms of the final frequency-amplitude relationship.
5) Accuracy of the proposed solution methods is sufficiently reliable for vibration analysis of FGM structure even for large amplitudes and presence of strong nonlinearity.
6) In the case of FGM beam with power law property variation, one can sort the relative error in different boundary condition to be: Relative error %: C-C < C-H < H-H.

Appendix 1.

The coefficients γ_a , γ_b, γ_c in Equation (14) are defined as:

$$\gamma_a = -\frac{d_0 \eta^2}{\Lambda_0} \int_0^1 \psi \frac{d^4 \psi}{d\zeta^4} d\zeta \ , \tag{1.1}$$

$$\gamma_b = \frac{b_{11} \eta^2}{\Lambda_0} \left(\int_0^1 \frac{d^2 \psi}{d\zeta^2} d\zeta \right) \int_0^1 \psi \frac{d^2 \psi}{d\zeta^2} d\zeta \ , \tag{1.2}$$

$$\gamma_c = \frac{a_{11} \eta^2}{\Lambda_0} \left(\int_0^1 \psi \frac{d^2 \psi}{d\xi^2} d\xi \right) \int_0^1 \left(\frac{d\psi}{d\xi} \right)^2 d\xi \ , \tag{1.3}$$

$$\Lambda_0 = \bar{I} \int_0^1 \psi \psi d\xi \ , \tag{1.4}$$

where $\gamma_a = \omega_l^2$. The values of these coefficients for different FGM beams are listed in the following Table 2. Let $\gamma_a = \alpha, \ \gamma_b = \beta, \ \gamma_c = \gamma$.

Appendix 2.

The system of Eq. (14) oscillates between $\left[-b, a\right]$ for positive a, b , when $u = a$ and $u = b$ one has $\dot{u} = 0$. Also, a is given by initial condition and b indicates unknown amplitude in negative direction to be determined. Setting $\gamma_a = \alpha, \gamma_b = \beta, \gamma_c = \gamma$ and multiplying $\dot{u}$ on both sides of Eq. (14):

$$\ddot{u}\dot{u} + \alpha u\dot{u} + \beta u^2\dot{u}^2 + \gamma u^3\dot{u} = 0. \tag{2.1}$$

Table 2. Dimensionless coefficients $\gamma_a(\times 10^{-2}), \gamma_b(\times 10^{-2})$ and $\gamma_c(\times 10^{-2})$ [17]

Exponential/ power law	H-H			C-C			C-H		
	γ_a	γ_b	γ_c	γ_a	γ_b	γ_c	γ_a	γ_b	γ_c
$\frac{E_2}{E_1} = 0.2$	3.2884	-2.9732	9.4166	14.383	0.0	11.720	7.0359	-2.2134	12.224
$\frac{E_2}{E_1} = 1.0$	3.1709	0.0	9.5126	16.294	0.0	11.720	7.7383	0.0	12.400
$\frac{E_2}{E_1} = 5.0$	3.2884	-2.9732	9.4166	14.383	0.0	11.720	7.0359	-2.2134	12.224
$n = 0.3$	0.8417	-0.1384	2.4821	4.3057	0.0	3.0591	2.0464	-0.1016	3.2354
$n = 1.0$	1.1938	-0.2935	3.5903	6.0727	0.0	4.4265	2.8889	-0.2155	4.6796
$n = 3.0$	1.7433	-0.3617	5.4284	8.8965	0.0	6.6912	4.2300	-0.2656	7.0755

By integrating the above expression one can arrive at:

$$\frac{1}{2}\dot{u}^2 + \frac{1}{2}\alpha u^2 + \frac{1}{3}\beta u^3 + \frac{1}{4}\gamma u^4 = C, \tag{2.2}$$

in which C is the integration constant. For the conservative system and substituting the conditions that $\dot{u} = 0$ when $u = a$ and $u = b$ one has:

$$\frac{1}{2}\alpha a^2 + \frac{1}{3}\beta a^3 + \frac{1}{4}\gamma a^4 = \frac{1}{2}ab^2 - \frac{1}{3}\beta b^3 + \frac{1}{4}\gamma b^4. \tag{2.3}$$

Solving the above equation, the exact value of b can be obtained for the given values of α, β, γ and a.

Appendix 3.

The first approximate frequency, period T and the corresponding periodic solution $u(t)$ of Eq. (14) are eventually presented by:

$$T_a = \frac{2\pi}{\omega_a},\ T_b = \frac{2\pi}{\omega_b} \Rightarrow T = \frac{T_a + T_b}{2} \quad \text{and} \quad \omega = \frac{2\pi}{T}, \tag{3.1}$$

$$u(t) = \begin{cases} a\cos\omega_a t, & \text{when } 0 \le t \le \frac{T_a}{4}, \\ b\cos\omega_b(t - \frac{T_a}{4} + \frac{T_b}{4}), & \text{when } \frac{T_a}{4} \le t \le \frac{T_a}{4}, \\ a\cos\omega_a(t + \frac{T_a}{2} - \frac{T_b}{2}), & \text{when } \frac{T_a}{4} + \frac{T_b}{2} \le t \le T. \end{cases} \tag{3.2}$$

References

[1] **Ichikawa K.** Functionally Graded Materials in the 21st Century: A Worksop on Trends and Forecasts. Kluwer Academic Publishers, Massachusetts, 2001.

[2] **Müller E., Drašar C., Schilz J., Kaysser W. A.** Functionally graded materials for sensor and energy applications. Materials Science and Engineering A, Vol. 362, Issue 1-2, 2003, p. 17–39.

[3] **Slowak R., Hoffmann S., Liedtke R., Waser R.** Functional graded high-K (Ba1-xSrx)TiO3 thin films for capacitor structures with low temperature coefficient. Integrated Ferroelectrics, Vol. 24, Issue 1-4, 1999, p. 169–179.

[4] **Gerk Ch., Willert-Porada M.** Powder metallurgical processing and properties of copper/tungsten gradients. Materials Science Forum, Vol. 308-311, 1999, p. 806–813.

[5] **Kaysser W. A.** Development of graded composite electrodes for the SOFC. Materials Science Forum, Vol. 308-311, 1999, p. 806–813.

[6] **Birth U., Joensson M., Kieback B.** Powder metallurgical processing and properties of copper/tungsten gradients. Materials Science Forum, Vol. 308-311, 1999, p. 766–773.

[7] **Loy C. T., Lam K. Y., Reddy J. N.** Vibration of functionally graded cylindrical shells. International Journal of Mechanical Sciences, Vol. 41, Issue 3, 1999, p. 309–324.

[8] **Yang J., Shen H. S.** Dynamic response of initially stressed functionally graded rectangular thin plates. Composite Structures, Vol. 54, Issue 4, 2001, p. 497–508.

[9] **Yang J., Kitipornchai S., Liew Large K. M.** Large amplitude vibration of thermo-electro-mechanically stressed FGM laminated plates. Computer Methods in Applied Mechanics and Engineering, Vol. 192, Issue 35-36, 2003, p. 3861–3885.

[10] **Chena C. S., Chena T. J., Chien R. D.** Nonlinear vibration of initially stressed functionally graded plates. Thin-Walled Structures, Vol. 44, Issue 8, 2006, p. 844–851.

[11] **Zhong Z., Yu T.** Vibration of a simply supported functionally graded piezoelectric rectangular plate. Smart Materials and Structures, Vol. 15, Issue 5, 2006, p. 1404–1412.

[12] **Zhang T. T., Shi Z. F., Spencer B. F.** Vibration analysis of a functionally graded piezoelectric cylindrical actuator. Smart Materials and Structures, Vol. 17, Issue 2, 2008, p. 025018.

[13] **Lu A., Chen C.** Free vibration of orthotropic functionally graded beams with various end conditions. Structural Engineering and Mechanics, Vol. 20, Issue 4, 2005, p. 465–476.

[14] **Wei D., Liu Y., Xiang Z.** An analytical method for free vibration analysis of functionally graded beams with edge cracks. Journal of Sound and Vibration, Vol. 331, Issue 7, 2012, p. 1686–1700.

[15] **Simsek M.** Non-linear vibration analysis of a functionally graded Timoshenko beam under action of a moving harmonic load. Composite Structures, Vol. 92, Issue 10, 2010, p. 2532–2546.

[16] **Pradhan S. C., Murmu T.** Thermo-mechanical vibration of FGM sandwich beam under variable elastic foundations using differential quadrature method. Journal of Sound and Vibration, Vol. 321, Issue 1-2, 2009, p. 342–362.

[17] **Ke L. L., Yang J., Kitipornchai S.** An analytical study on the nonlinear vibration of functionally graded beams. Meccanica, Vol. 45, Issue 6, 2010, p. 743–752.

[18] **Laia S. K., Harrington J., Xiang Y., Chow K. W.** Accurate analytical perturbation approach for large amplitude vibration of functionally graded beams. International Journal of Non-Linear Mechanics, Vol. 47, Issue 5, 2012, p. 473–480.

[19] **Janghorban M., Zare A.** Thermal effect on free vibration analysis of functionally graded arbitrary straight-sided plates with different cutouts. Latin American Journal of Solids and Structures, Vol. 8, Issue 7, 2011, p. 245–257.

[20] **Rahimi G. H., Ansari R., Hemmatnezhad M.** Vibration of functionally graded cylindrical shells with ring support. Scientia Iranica, Vol. 18, Issue 6, 2011, p. 1313–1320.

[21] **Behjat B., Salehi M., Armin A., Sadighi M., Abbasi M.** Static and dynamic analysis of functionally graded piezoelectric plates under mechanical and electrical loading. Scientia Iranica, Vol. 18, Issue 4, 2011, p. 986–994.

[22] **Arefi M., Rahimi G. H.** Comprehensive thermoelastic analysis of a functionally graded cylinder with different boundary conditions under internal pressure using first order shear order deformation theory. Mechanika, Vol. 18, Issue 1, 2012, p. 5–13.

[23] **He J. H.** Homotopy perturbation method for bifurcation of nonlinear problems. International Journal of Nonlinear Science and Numerical Simulation, Vol. 6, Issue 2, 2005, p. 207–208.

[24] **He J. H.** The homotopy perturbation method for nonlinear oscillators with discontinuities. Applied Mathematics and Computation, Vol. 151, Issue 1, 2004, p. 287–292.

[25] **He J. H.** Application of homotopy perturbation method to nonlinear wave equations. Chaos, Solitons & Fractals, Vol. 26, Issue 3, 2005, p. 695–700.

[26] **Younesian D., Askari H., Saadatnia Z., Kalami Yazdi M.** Free vibration analysis of strongly nonlinear generalized Duffing oscillators using He's variational approach & homotopy perturbation method. Nonlinear Science Letters A, Vol. 2, Issue 1, 2011, p. 11–16.

[27] **He J. H.** An improved amplitude-frequency formulation for nonlinear oscillators. International Journal of Nonlinear Sciences and Numerical Simulation, Vol. 9, Issue 2, 2008, p. 211–212.

[28] **Younesian D., Askari H., Saadatnia Z., Yazdi M. K.** Frequency analysis of strongly nonlinear generalized Duffing oscillators using He's frequency_amplitude formulation and He's energy balance method. Computers and Mathematics with Applications, Vol. 59, Issue 9, 2010, p. 3222–3228.

[29] **Kalami Yazdi M., Khan Y., Madani M., Askari H., Saadatnia Z., Yildirim A.** Analytical solutions for autonomous conservative nonlinear oscillator. International Journal of Nonlinear Sciences and Numerical Simulation, Vol. 11, Issue 11, 2010, p. 979–984.

[30] **Askari H., Saadatnia Z., Younesian D., Yildirim A., Kalami Yazdi M.** Approximate periodic solutions for the Helmholtz–Duffing equation. Computers & Mathematics with Applications, Vol. 62, Issue 10, 2011, p. 3894–3901.

[31] **Khan Y., Kalami Yazdi M., Askari H., Saadatnia Z.** Dynamic analysis of generalized conservative nonlinear oscillator via frequency amplitude formulation. Arabian Journal for Science and Engineering, 2011, DOI: 10.1007/s13369-011-0035-y.

[32] **Kovacic I., Brennan M. J.** The Duffing Equation Nonlinear Oscillators and Their Behaviour. New York: Wiley, 2011.

[33] **Mickens R. E.** A generalization of the method of harmonic balance. Journal of Sound and Vibration, Vol. 111, Issue 3, 1986, p. 515–518.

[34] **Yildirim A., Askari H., Kalami Yazdi M., Khan Y.** A Relationship Between Three Analytical Approaches to Nonlinear Problems. 2012, DOI:10.1016/j.aml.2012.02.001.

[35] **Sedighi H. M., Shirazi K. H.** A new approach to analytical solution of cantilever beam vibration with nonlinear boundary condition. ASME Journal of Computational and Nonlinear Dynamics, Vol. 7, Issue 3, 2012, p. 034502, DOI:10.1115/1.4005924.

[36] **Sedighi H. M., Reza A., Zare J.** Dynamic analysis of preload nonlinearity in nonlinear beam vibration. Journal of Vibroengineering, Vol. 13, Issue 4, 2011, p. 778–787.

[37] **Sedighi H. M., Reza A., Zare J.** Analytical approximation of nonlinear frequency of cantilever beam vibrations. Journal of Vibroengineering, Vol. 14, Issue 1, 2012, p. 270–279.

[38] **Sedighi H. M., Shirazi K. H., Reza A., Zare J.** Accurate modeling of preload discontinuity in the analytical approach of the nonlinear free vibration of beams. Proceedings of the Institution of Mechanical Engineers, Part C: Journal of Mechanical Engineering Science, 2012, DOI: 10.1177/0954406211435196.

[39] **Bayat M., Pakar I., Bayat M.** Analytical study on the vibration frequencies of tapered beams. Latin American Journal of Solids and Structures, Vol. 8, Issue 2, 2011, p. 149–162.

[40] **Ghadimi M. A., Kaliji H. D., Barari A.** Analytical solutions to nonlinear mechanical oscillation problems. Journal of Vibroengineering, Vol. 13, Issue 2, 2011, p. 133–143.

[41] **Pakar I., Bayat M., Bayat M.** On the approximate analytical solution for parametrically excited nonlinear oscillators. Journal of Vibroengineering, Vol. 14, Issue 1, 2012, p. 423–429.

[42] **Pakar I., Bayat M.** Analytical study on the non-linear vibration of Euler-Bernoulli beams. Journal of Vibroengineering, Vol. 14, Issue 1, 2012, p. 216–224.